

**THE GEOMETRY OF THE TYRAS VALLIS FAN: USING STRATIGRAPHY TO STUDY DEPOSITIONAL ENVIRONMENT.** M. A. Tebolt<sup>1</sup> and T. A. Goudge<sup>1</sup>, <sup>1</sup>Jackson School of Geosciences, University of Texas at Austin. (Contact: mtebolt@utexas.edu)

**Background:** Sedimentary rocks record conditions about the environment in which they were deposited. Through the use of orbital data, it is possible to examine sedimentary fan features on the surface of Mars to understand their depositional environment and constrain the amount of water that was present on the surface [e.g., 1-3]. Previous studies have examined the geomorphology of the fans alone to infer the depositional environment [e.g., 4-6], but this method has limitations. Billions of years of erosion may have significantly altered the geomorphology of a fan deposit; however, the overall stratigraphy, or internal architecture, of a fan deposit will remain preserved.

Here, we consider the stratigraphy of a fan feature at the mouth of Tyras Vallis to evaluate if the depositional setting was subaerial or lacustrine. If the layers of the fan have relatively consistent dip from the mouth of the valley to the toe, this would be indicative of subaerial deposition in an alluvial fan [7,8]. Alternatively, if the layer dips have slope breaks from shallow to steep and/or steep to shallow from the proximal to distal end of the fan, this is more indicative of a delta clinoform shape that was deposited into a standing lake [9,10]. Using fan stratigraphy to constrain the presence or absence of long standing bodies of water can help contribute to the understanding of the ancient climate of the Tyras Vallis region at the time of deposition.

**Description of Tyras Fan:** The Tyras fan extends from the mouth of Tyras Vallis down the northwest wall of an unnamed crater (8.42°N, -49.71°E). The crater is Noachian in age [11] and is ~70 km in diameter. It is located near the martian dichotomy in the Xanthe Terra region. The fan has previously been interpreted as a delta with significant wave erosion that formed during lake retreat and two lake highstands at 700 and 550 m [12].

The Tyras fan has three morphologically distinct units separated by two scarps (Fig. 1). The upper unit, Unit 1, extends ~4.5 km into the crater and has prominent layers exposed on the surface as topographic benches (Fig. 1), particularly within a series of ~500 m wide U-shaped incisions that extend 1-2 km downslope (Fig. 1A). A scarp with no visible exposed internal structure separates Unit 1 from Unit 2. Unit 2 extends to ~7 km into the crater, the layers are not as prominent as they are in the upper unit, resulting in fewer identifiable layers. The scarp between Unit 2 and Unit 3 is shedding boulders and has bands with tone differences on the scarp face that we interpret as internal layering. The lower unit extends to ~25 km into the crater and

has a more degraded texture with fewer visible layers than the stratigraphically higher units.

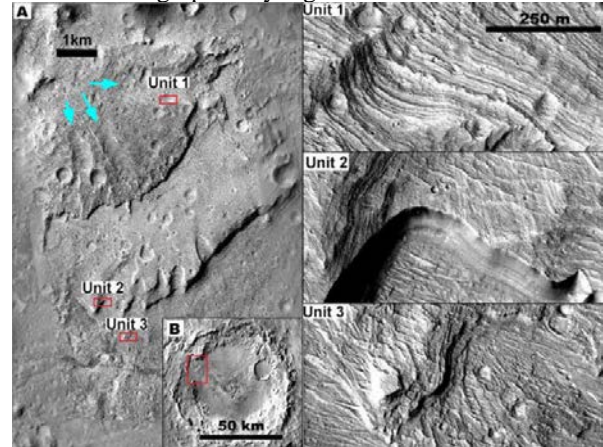


**Fig. 1.** HiRISE and CTX images of the Tyras fan. (A) HiRISE image PSP\_008167\_1885 of the Tyras fan, the upper, middle, and lower unit are visible as Unit 1, 2, and 3. The blue arrows point towards U-shaped incisions with prominent exposed layers. The images on the right show the layers mapped within each unit. (B) CTX mosaic [13] of the entire crater.

**Methods:** A total of 674 layers were mapped on the Tyras fan using HiRISE image PSP\_008167\_1885 with a resolution of ~25 cm/px. We mapped each layer only if it was recognized as a topographic bench, or as a horizontal band of tone change on the face of the scarps. The elevation and position of the layers (at 2 m intervals) were extracted from a DEM constructed from HiRISE images PSP\_008167\_1885 and PSP\_008602\_1885 using the open source NASA Ames Stereo Pipeline (ASP) [14,15]. This spatial data was used to fit a plane to each layer. Five checks were performed to filter out low quality layer fits. The first check is based on the collinearity of the points; using a principal component analysis (PCA), if more than 99.5% of the variability is expressed by principal component 1, there is too much uncertainty and the layer was rejected [16]. The second check examined the vertical variance of the points about the best-fit layer; if variance in principal component 2 is less than 15x greater than the variance in principal component 3, the layer was rejected [16]. Next, any layers with a root mean squared error greater than 1 m were rejected, along with any layers shorter than 100 m. Finally, if any of the planes were not generally dipping towards the center of the basin, they were rejected.

**Results:** Of the original 674 layers mapped, 112 passed all of the checks and were determined to be fit for analysis (Fig. 2). Of these 112 layers, 77 were

mapped on Unit 1, 25 on Unit 2, and 10 on Unit 3. The average dip of each layer was  $2.1^\circ$  for Unit 1,  $2.4^\circ$  for Unit 2, and  $2.3^\circ$  for Unit 3. Projecting each of these units out with their respective average slopes, they meet the crater floor at  $\sim 13$  km,  $\sim 14$  km, and  $\sim 19.5$  km into the basin with respect to the valley mouth at the crater rim. The majority of the layers are shallow, with about  $\frac{2}{3}$  of the layers dipping below  $3^\circ$ .

The range of the dips in Unit 1 gradually increase moving further out towards the basin. The dips range from  $<1^\circ$  to  $4^\circ$  in the first kilometer away from the valley mouth and increase towards the toe of the first unit ending with a range from  $<1^\circ$  to  $\sim 8^\circ$ , with one outlier  $>10^\circ$ . The dips of Unit 2 and 3 stay relatively consistent ranging from  $<1^\circ$  to  $\sim 6^\circ$  (Fig. 2).

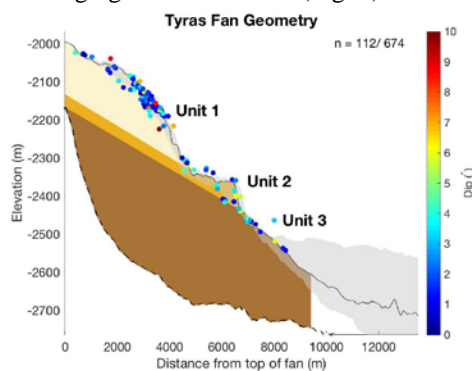


**Fig. 2.** Stratigraphy of the Tyras fan. 112 layers are plotted as points with color representing the dip of the layer. The surface of the fan was calculated by taking the median elevation of 7 profiles of the fan. The gray area is the 25<sup>th</sup>-75<sup>th</sup> percentile range of the elevation. The base of Unit 3 is estimated from the profile of the crater wall  $\sim 5$  km NW from the fan.

**Discussion:** Most of the characteristics of the fan layer geometry are consistent with an alluvial fan, but some results leave room for a deltaic interpretation. All three units of the fan have generally shallow and relatively constant slopes from proximal to distal end, consistent with the geometry of an alluvial fan [7,8]. Additionally, when these layers are projected into the basin at a constant slope, topographic features are found at the locations where the units would intersect the crater floor, which may be eroded remnants of the original toe of the fan. Projecting the units out at an average constant slope should provide a reasonable estimate for the position of the toe of an alluvial fan. However, if this method was used to estimate the original horizontal length of a delta, it would overestimate the fan's length due to the slope breaks in the clinoform shape. The fan has undergone a great deal of erosion so it is possible that it originally extended all the way out to the topographic features, even in a deltaic environment. Taken together, our observations generally point towards a subaerial depositional environment, rather than a deltaic environment, for the Tyras fan.

When examining the data, it is important to consider the amount of erosion that has impacted the fan. Although modern erosion rates on Mars are much less than those on Earth [17], the Tyras fan has likely experienced billions of years of erosion [18]. This has significantly changed the geomorphology of the fan from when it was originally deposited. If the topographic features found nearly 20 km downslope from the valley mouth are remnants of the original distal end of the fan, this would mean that over half of the material has been removed from the fan and that the scarps at the toe of each unit are erosional features. Indeed, the mere fact that this fan exposes internal layering (Fig. 1) points to significant erosion of the outcrop.

The dips of the fan are generally constant, but the increase of the dip range in Unit 1 is of particular interest. The dips generally become steeper from proximal to distal end of the unit. This may represent a slope break, which could indicate that the top unit was deposited in a deltaic environment. This trend is not observed in the other two units, so if the depositional environment is responsible for these dip values, it is unique to Unit 1. Ongoing analyses will further test this hypothesis.

To continue this study, we are conducting the same stratigraphic analysis on other fan features across Mars. The results will be used to constrain the size, location, and timing of water reservoirs across the martian surface, which will contribute to the understanding of the ancient climate of Mars.

**References:** [1] Lewis, K. W., Aharonson, O. (2006) *Journal of Geophysical Research: Planets*, vol. 111, no. E6. [2] DiBiase, R. A., et al. (2013) *Journal of Geophysical Research: Planets*, vol. 118, no. 6, pp. 1285–302. [3] Goudge, T. A., et al. (2017) *Earth and Planetary Science Letters*, vol. 458, pp. 357–65. [4] Di Achille, G., Hynes B. M. (2010) *Nature Geoscience*, vol. 3, no. 7, pp. 459–63. [5] Bhattacharya, J. P., et al. (2005) *Geophysical Research Letters*, vol. 32, no. 10. [6] Ori, G. G., et al. (2000) *Journal of Geophysical Research: Planets*, vol. 105, no. E7, pp. 17629–41. [7] Bull, W. B. (1977) *Prog. Phys. Geogr.* [8] Blair, T.C., McPherson J.G. (1994) *J. Sediment.* [9] Jr, R. M. Mitchum, et al. (1977) *Seismic Stratigraphy and Global Changes of Sea Level*, pp. 117–33. [10] Rich, J. L. (1951) *GSA Bulletin*, vol. 62, no. 1, pp. 1–20. [11] Scott, D. H., Tanaka, K. L. (1986), *Geologic map of the western equatorial region of Mars*, U.S. Geol. Surv. Misc. Invest. Ser. Map, I-1802–A. [12] Di Achille, G. et al. (2006) *Journal of Geophysical Research: Planets*, vol. 111, no. E4. [13] Dickson, L.A. et al. (2018) *LPI Contrib. No. 2083*. [14] Beyer, R. A., et al. (2018) *Earth and Space Science*, vol. 5, no. 9, pp. 537–48. [15] Shean, et al. (2016) *ISPRS Journal of Photogrammetry and Remote Sensing*, vol. 116, pp 101-117. [16] Lewis, K. W., et al. (2008) *Journal of Geophysical Research: Planets*, vol. 113, no. E12. [17] Golombek, M. P., et al. (2014) *Journal of Geophysical Research: Planets*, vol. 119, no. 12, pp. 2522–47. [18] Hauber, E., et al. (2018) *Journal of Geophysical Research: Planets*, pp. 1529–44.